ISSN 1024-8560, Atmospheric and Oceanic Optics, 2017, Vol. 30, No. 2, pp. 162–168. © Pleiades Publishing, Ltd., 2017.
Original Russian Text © V.V. Vorob'ev, 2016, published in Optika Atmosfery i Okeana.

REMOTE SENSING OF ATMOSPHERE, HYDROSPHERE, AND UNDERLYING SURFACE

On the Applicability of Asymptotic Formulas of Retrieving "Optical" Turbulence Parameters from Pulse Lidar Sounding Data: II—Results of Numerical Simulation

V. V. Vorob'ev†

Obukhov Institute of Atmospheric Physics, Russian Academy of Sciences, Moscow, 119017 Russia
e-mail: psb@iao.ru

Received June 2, 2016

Abstract—The applicability of formulas derived in the first part of this work has been studied in a numerical experiment. The geometrical optics approximation is shown to be applicable only on short paths whose length is less than the corresponding diffraction lengths by a factor of hundreds. The restrictions are caused by oscillations of the kernel of the initial integral equation. They lead to strong oscillations of the third derivative of the measured data. The formulas based on the asymptotic formula of the kernel for a point receiver are slightly sensitive to oscillations of the measured data. Applying the formulas for a point receiver in the case of receivers with a finite radius smoothes the retrieved distributions and shifts them with respect to the given ones. A technique of taking these factors into account in the process of retrieving has been proposed. Together with smoothing of the retrieved distributions, applying the point receiver approximation leads to partial loss of the information about the turbulence spectrum in the retrieved data. This allows one to simplify the retrieval procedure by reducing it to calculating usual derivatives of the second order.

Keywords: lidars, turbulence, backscattering enhancement, Volterra and Abel equations
DOI: 10.1134/S1024856017020142

INTRODUCTION

In the first part of this work [1], asymptotic solutions were found for the integral equation of the relation between the distribution of the structure characteristic of refractive index fluctuations along a lidar sounding path and backscattering enhancement factor. The statement of the problem was considered in detail in [1] and corresponds to theoretical investigations [2, 3] and experiments [4, 5]. The asymptotic solutions are reduced to finding usual or fractional derivatives of the measured quantities. This paper presents results of the numerical study concerning the applicability range of the asymptotic solutions and simple modifications of the retrieval formulas for expanding the ranges of their applicability.

The technique of studying the applicability ranges is trivial. For a given distribution of the normalized structure parameter $y(x) = \hat{C}^2_{n,\gamma}(x)\big/\hat{C}^2_{n,\gamma}(0)$, the measured quantity, i.e., the enhancement factor of the received power $q(x)$, is calculated by the formula

$$q(x) = \int_0^x K(x,\xi)y(\xi)d\xi, \qquad (1)$$

where $K(x,\xi)$ denotes the function (the kernel of the integral equation)

$$K(x,\xi) = A\int_0^\infty \kappa_\perp^{-\gamma}\left\{1-\cos\left(\frac{\xi(x-\xi)}{k_0 x}\kappa_\perp^2\right)\right\} \times \frac{x}{\xi R}J_1\left(\frac{\xi R}{x}\kappa_\perp\right)d\kappa_\perp. \qquad (2)$$

Here, $A = 16\pi^2 k_0^2 \hat{C}^2_{n,\gamma}(0)$ is constant, $k_0 = 2\pi/\lambda$, λ is the light wavelength; R is the radius of the receiving aperture; and J_1 is the Bessel function. As was shown in [1], the function $K(x,\xi)$ in the general case is a complicated oscillating function.

Then, using the function $q(x)$, the function $Y(x)$ is retrieved by the asymptotic formulas. It is denoted by a capital letter to distinguish it from the given one. The applicability of the approximate formulas is estimated by differences between the functions $Y(x)$ and $y(x)$.

1. GEOMETRICAL OPTICS APPROXIMATION

The solution of the inverse problem in the geometrical optics approximation is defined by the relation [1]:

$$y(x)B_g(R) = \frac{1}{x^{\gamma-4}}\frac{d^3}{dx^3}\left(x^{\gamma-4}q(x)\right), \qquad (3)$$

† Deceased.

where γ is the power index of the three-dimensional spectrum $\left(\Phi_n(\kappa) \sim \kappa^{-\gamma}\right)$ of refractive index fluctuations; the quantity $B_g(R)$ is defined by formulas (20) and (25) in [1].

Since the measured quantity $q(x)$ can vary within a broad range, it is more convenient to pass to the function $f(x) = q(x)/q_{0,0}(x)$, where $q_{0,0}(x)$ is the backscattering enhancement factor in a statistically homogeneous medium ($y = 1$); the factor is calculated in the geometrical optics approximation:

$$q_{0,0}(x) = \int_0^{x_n} K_g(x,\xi)d\xi = B_g \cdot v(\gamma)x^3,$$
$$v(\gamma) = \frac{2}{(\gamma-3)(\gamma-2)(\gamma-1)}, \quad (4)$$

($K_g(x,\xi) = B_g\left[\frac{\xi}{x}\right]^{(\gamma-4)}(x-\xi)^2$ is the geometrical optics approximation of the kernel [1]).

Then, the following relation follows from (3) and (4) for the function $f(x)$:

$$Y(x) = \frac{v(\gamma)}{2}x^{4-\gamma}\frac{d^3}{dx^3}\left[x^{\gamma-1}f(x)\right]$$
$$= f(x) + \frac{3}{\gamma-3}x\frac{df}{dx} + \frac{3}{(\gamma-3)(\gamma-2)}x^2\frac{d^2f}{dx^2} \quad (5)$$
$$+ \frac{1}{(\gamma-3)(\gamma-2)(\gamma-1)}x^3\frac{d^3f}{dx^3}.$$

In all the examples considered below, the derivatives of the functions were calculated by the formulas

$$f_n' = \frac{1}{2\Delta}(f_{n+1} - f_{n-1}), \quad f_n'' = \frac{1}{2\Delta}(f_{n+1}' - f_{n-1}'),$$
$$f_n''' = \frac{1}{2\Delta}(f_{n+1}'' - f_{n-1}''), \quad (6)$$

where $f_n = f(x_n)$, $f_{n\pm1} = f(x_n \pm \Delta)$; and Δ is the sampling interval in the coordinate x.

First, the simplest model was considered: $y(x) = 1$. The retrieval results for three values of the aperture radius are shown in Fig. 1.

It is seen that the geometrical optics asymptotics poorly operates in the retrieval problem. The functions $Y(x, R)$ presented in this figure decrease with the distance approximately as $Y(x) \approx \exp\left[-25x/(k_0R^2)\right]$. Correspondingly, the systematic error of retrieving exponentially grows with the distance.

In the case $y(x) = 1$, this error can be eliminated if the function $q_{0,0}(x)$ which is calculated in the geometrical optics approximation is replaced in the determination of the function $f(x)$ by $q_0(x) = \int_0^x K(x,\xi)d\xi$ which takes into account the influence of diffraction,

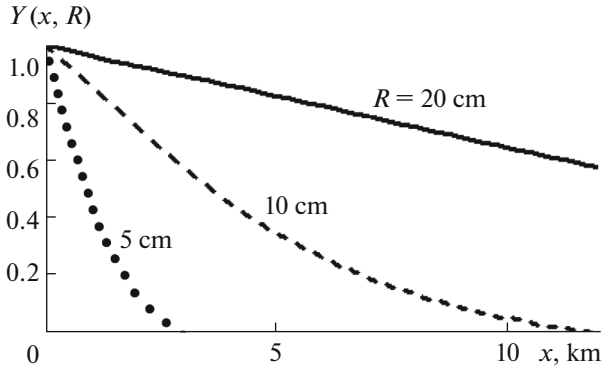

Fig. 1. Retrieved distributions $Y(x)$ for the given $y(x) = 1$ and three values of the aperture radii shown near the curves. The calculation parameters are $\lambda = 0.532$ μm, $\gamma = 11/3$, and $\Delta = 250$ m.

i.e., by setting $f(x) = q(x)/q_0(x)$. If $y(x) = 1$, $f(x) = 1$ and, according to (5), $Y(x) = 1$.

Then, it was investigated whether formula (5) with $f(x) = q(x)/q_0(x)$ is applicable for retrieving the stepwise distribution $y(x)$ of the form

$$y(x) = 1 + \exp\left[-\left(\frac{x - X_0 - H}{H}\right)^{20}\right]$$
$$\text{for } x \le X_0 + H,$$
$$y(x) = 2 \text{ for } x > X_0 + H, \quad (7)$$
$$\text{with } H = 100 \text{ m}.$$

The retrieval examples are presented in Fig. 2. The calculations were carried out for a turbulence model with the spectrum index $\gamma = 11/3$.

Figure 2 shows errors which can be made by using the geometrical optics asymptotics. It is interesting that the structure of retrieval errors as functions of the coordinate x is oscillating, by analogy with the structure of functions $u(Q)$ presented in Fig. 3 in [1]. As seen from Fig. 2, the function $y(x)$ is retrieved correctly after the jump point X_0 only on a certain interval L_g marked in the upper figures by a double bar. At $R =$ 10 cm and a small value of the half-width of the smoothing window $S = 20$ m, the interval L_g slightly depends on the coordinate X_0. It increases from 0.4 (at $X_0 = 0.2$ km) to 0.5 km (at $X_0 = 1.2$ km). When the data are smoothed, the applicability interval of the retrieval formulas L_g increases approximately by the half-width S of the smoothing window. For a window half-width $S = 200$ m, the interval L_g correspondingly varies from 0.6 to 0.8 km. At values of the receiving aperture radius $R = 5$ and 20 cm, the interval L_g, as was elucidated, depends on R approximately linearly and varies at $S =$ 200 m and $x = 0.25$–2 km within $L_g = 0.35$–0.4 km at $R = 5$ cm and $L_g = 1.1$–1.6 km at $R = 20$ cm.

Figure 3 shows how formulas of the geometrical optics approximation operate in the case of more com-

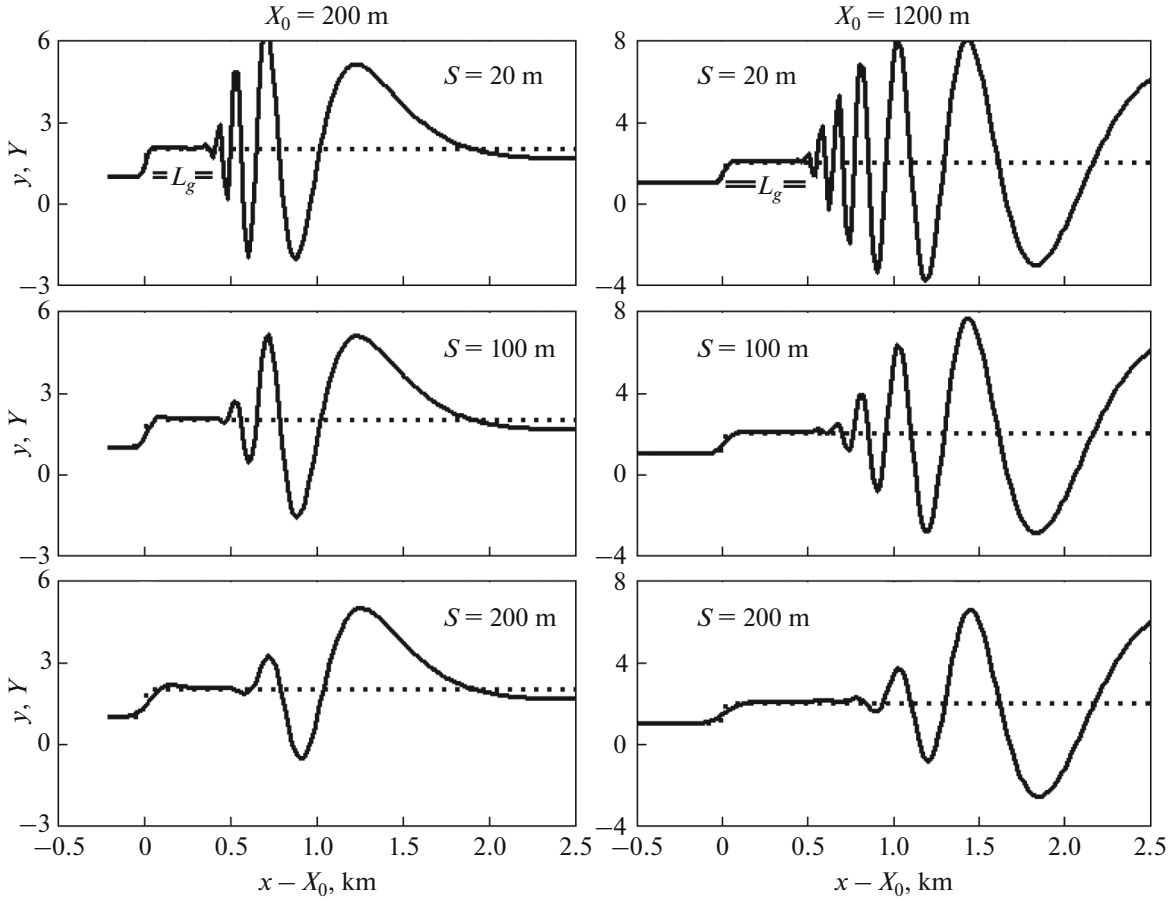

Fig. 2. Distributions $y(x)$ and $Y(x)$ specified by formula (7) (dotted lines) and retrieved ones (solid curves) at the aperture radius $R = 10$ cm. The distances X_0 from the jump of the distribution $y(x)$ are equal to 200 m for the left column and to 1200 m for the right column. The sampling interval was chosen to be $\Delta = 20$ m. The half-width S of the Gaussian smoothing window for the data f_n is shown near the plots.

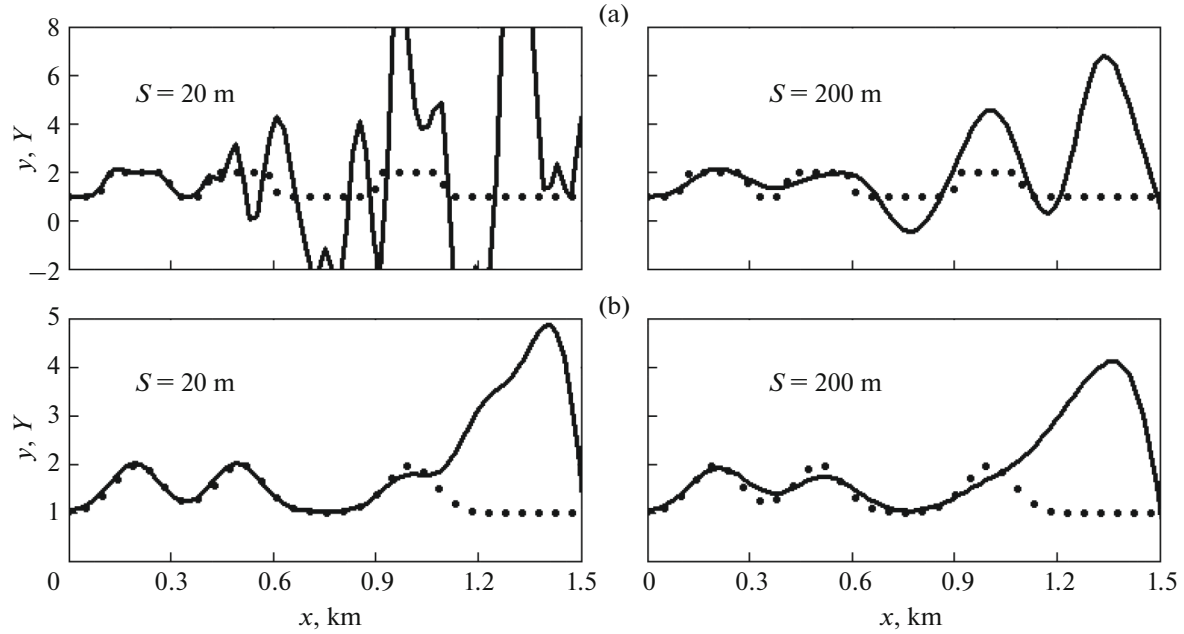

Fig. 3. Given distributions y (dotted lines) and distributions Y retrieved in the geometrical optics approximation (solid curves) for the case of (a) super-Gaussian layers (8) with $m = 20$ and (b) Gaussian layers. The calculation parameters are $R = 10$ cm, $\lambda = 0.532$ μm, $\gamma = 11/3$, and $\Delta = 20$ m. The figures show half-widths of the smoothing windows S.

plicated distributions $y(x)$. The distributions $y(x)$ in calculations of Fig. 3 were specified in the form

$$y(x) = 1 + \sum_{n=1}^{3} \exp\left(-\frac{(x - X_n)^m}{H^m}\right) \quad (8)$$

with $H = 100$ m, $X_{1;2;3} = 0.2$; 0.5; and 1 km

and with the index $m = 20$ (super-Gaussian layers) and $m = 2$ (Gaussian layers).

It is seen from Fig. 3a that only one and a half layers are resolved in the case of layers with steep boundaries in the absence of smoothing ($x \le 0.4$ km); in the case of smoothing by a window with $S = 200$ m, two layers ($x \le 0.6$ km), as for a single jump. Smooth Gaussian layers are resolved on a larger interval of $x \le 1$ km; in this case, the data smoothing is not required.

The performed calculations allow one to conclude that the applicability range of the geometrical optics asymptotics is narrow. For most commonly used lidars with receiving aperture radii of about 10 cm, the retrieval is possible at sounding distances not exceeding 0.5–1 km. An additional restriction upon the applicability can be caused by measurements noise which was not taken into account in the calculations.

2. POINT RECEIVER APPROXIMATION

The solution of the inverse problem in the point receiver approximation is defined by relation (23) in [1]:

$$Y(x)B_p(\gamma) = \frac{1}{x^\alpha}\frac{d}{dx}\int_0^x \frac{d}{d\xi}\left(\xi^\alpha q(\xi)\right)\frac{d\xi}{(x-\xi)^\alpha}. \quad (9)$$

The applicability of formula (9) was verified in the same way as the verification of the geometrical optics approximation. Namely, the function $q(x)$ was calculated by formulas (1) and (2); the retrieved function $Y(x)$, by formula (9). Let us denote

$$f(x) = q(x)\big/q_{p,\,0,0}(x), \quad (10)$$

where

$$q_{p,\,0,0}(x) = \int_0^x K_p(x,\xi)d\xi \quad (11)$$

($K_p(x,\xi)$ is the approximate kernel for the point receiver).

Relations (9) and (11) for the function $f(x)$ yield the formula

$$Y(x) = \frac{1}{w_0}\left(w(x) + \frac{2}{\gamma}x\frac{dw(x)}{dx}\right), \quad (12)$$

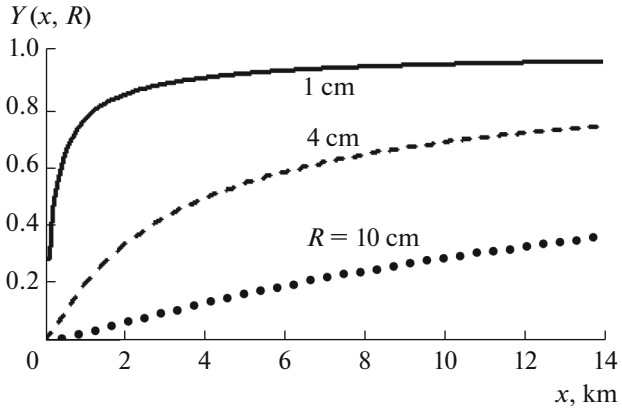

Fig. 4. Distributions $Y(x, R)$ retrieved by formulas (12) and (13) for the given $y(x) = 1$. Values of the radii R are shown near the plots. The calculation parameters are $\gamma = 11/3$ and $\Delta = 100$ m.

where

$$w_0 = \int_0^1 t^{\gamma-2}(1-t)^{1-\gamma/2}dt,$$

$$w(x) = \int_0^1 t^{\gamma-2}(1-t)^{1-\gamma/2} \quad (13)$$

$$\times\left[f(x\cdot t) + \frac{x\cdot t}{\gamma-1}\frac{df(x\cdot t)}{d(x\cdot t)}\right]dt.$$

Some results of the numerical calculations are presented in Figs. 4–8. Figure 4 shows retrieval results for the function $y(x) = 1$. Here, definitions (10) and (11) of the function $f(x)$ were used. It is seen that the retrieval accuracy is not high even in the case with an aperture with a radius of 1 cm. The retrieval accuracy can be improved in the same way as in the case of geometrical optics, namely, by normalizing the function $q(x)$ to the function $q_0(x) = \int_0^x K(x,\xi)d\xi$ which determines fluctuations at a finite size receiver in a homogenous medium.

Figure 5 shows examples of retrieving a stepwise distribution $y(x)$ of the form

$$y(x) = 1 + \exp\left(-\frac{(x - X_0 - H)^{20}}{H^{20}}\right) \quad \text{for } x \le X_0 + H;$$
$$y(x) = 2 \text{ for } x > X_0 + H \quad (14)$$

with $H = 100$ m, for three values of X_0 equal to 0.5, 1.5, and 2.5 km, and for three values of the radius R.

The first thing that is seen in Fig. 5 is the appearance of oscillations of the retrieved distribution after the jump in the initial distribution $y(x)$. They are detectable even at $R = 2$ cm and clearly seen at $R = 4$ cm. These oscillations, in contrast to those when using geometri-

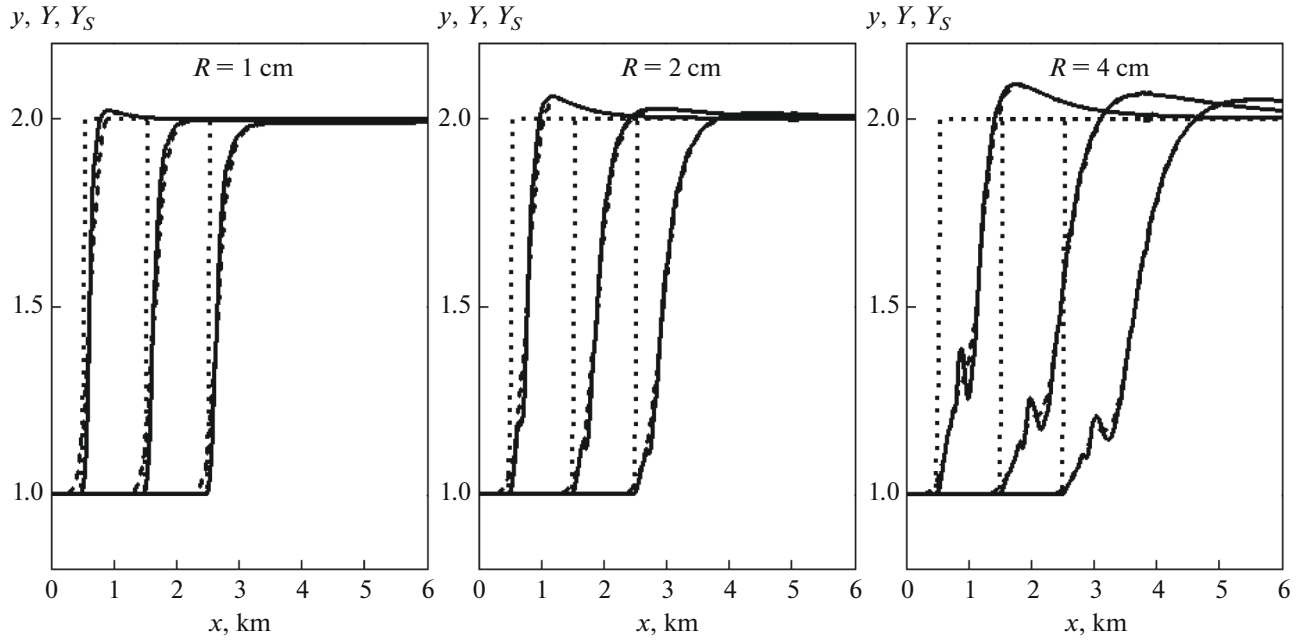

Fig. 5. Distributions: $y(x)$, specified by formula (12) (dotted lines); $Y(x)$, retrieved by formulas (12) and (13) with the function $f(x) = q(x)/q_0(x)$ (solid curves); and $Y_S(x)$, functions $Y(x)$ smoothed by a Gaussian window with a half-width of 300 m (dashed curves). The calculation parameters are $\gamma = 11/3$, $\Delta = 25$ m, and $H = 100$ m. Values of the aperture radii R are shown near the plots.

cal optics retrieval formulas, are removed by simple smoothing.

The main difference between the retrieved distributions and initial ones is the smearing of the jump boundary in the retrieved distribution; the smearing is as large as the radius of the receiving aperture and distance from the receiver to the jump boundary are large. For the half-width of the region over which the jump is smeared, one can take the shift $dX_0(X_0)$ which is determined by the equation $Y_S(X_0 + dX_0) = 1.5$. Here, Y_S is the distribution Y smoothed with a Gaussian window with a half-width S. Figure 6 shows the dependences $dX_0(X_0)$ calculated for $S = 300$ m for four values of the radius R.

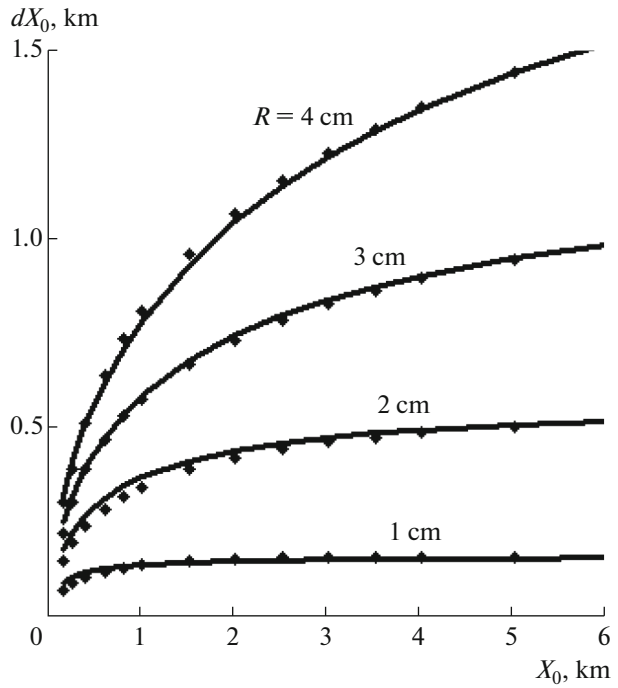

Fig. 6. Dependences of the shift dX_0 on the jump coordinate X_0 and radius R. The rhombuses are calculated points; the solid curves are approximate dependences (15).

The shift $dX_0(X_0, R)$ increases with both in the aperture radius R and coordinate X_0. Satisfactory approximations of the dependences $dX_0(X_0, R)$ in Fig. 6 are

$$dX_0(X_0, R) = 2.6[X_0 \cdot l(R)]^{1/2}\left(1 + \frac{X_0}{C_R L_d(R)}\right)^{-1/2}, \quad (15)$$

where the length dimension parameters are defined as $l(R) = k_0^{0.6}R^{1.6}$ and $L_d(R) = k_0 R^2$. The values of the dimensionless coefficient C_R at $R = 1$, 2, 3, and 4 cm are $C_R = 0.28$, 0.31, 0.33, and 0.4, respectively.

Figure 7 shows an example of retrieving a complicated distribution consisting of three Gaussian layers:

$$y(x) = 1 + \sum_{n=1}^{3} \exp\left(-\frac{(x - X_n - H)^2}{H^2}\right), \quad (16)$$

with the coordinates $X_1 = 500$ m, $X_2 = 2000$ m, $X_3 = 3500$ m, and layer half-width $H = 250$ m.

It is seen that the retrieved distributions differ from the given ones in the presence of a shift of maxima and minima and in smoothing of the initial distributions.

One can suppose that the shifts $dX(X, R)$ of the retrieved layers in the case under consideration are approximately the same as in the example with a jump-like distribution, i.e., they are determined by formula (15) with the argument X instead of X_0. The smoothing is also determined by a window with a half-width approximately equal to $dX(X, R)$. The results of verifying the hypothesis are illustrated by Fig. 8.

The smoothed functions $y_S(x)$ shown in Fig. 8 by dashed curves were calculated using the procedure of smoothing with a Gaussian window with a variable width. The half-width of the smoothing window as a function of x was specified to be proportional to the shift $dx(x, R)$, i.e., $S_y(x, R) = K_S(R)|dx(x, R)|$, where $K_S(R)$ is a dimensionless factor on the order of unity. It was chosen from the condition of the best visual coincidence of the retrieved and smoothed distributions $Y_S(x)$ and $y_S(x)$. For $R = 2$, 3, and 4 cm, the values of K_S are correspondingly 1.5, 1.1, and 0.9.

The retrieved distributions Y_S are depicted as functions of the argument $\tilde{x}$, taking into account the shift and defined as

$$\tilde{x}(x, R) = x - dX(x, R) + \delta(R). \qquad (17)$$

Here, $\delta(R)$ is the correction selected in the same way as the factor $K_S(R)$. Its values at $R = 0.02$, 0.03, and 0.04 m are $\delta = 50$, 100, and 200 m, respectively. The values of the corrections for the shift are lower approximate by a factor of ten than the shift (compare with Fig. 6).

The comparison of the distribution retrieved by the formulas for a point receiver and the smoothed initial distribution demonstrates their satisfactory agreement.

In the end of this section, one should note an interesting result found when solving the inverse problem of remote sounding of turbulence with a power index γ of the three-dimensional spectrum equal to 4. Instead of formulas (12) and (13), one can retrieve the distribution $Y(x)$ in this case by the function $f(x)$ in terms of usual derivatives:

$$Y(x) = f(x) + x\frac{df(x)}{dx} + \frac{1}{6}x^2\frac{d^2f(x)}{dx^2}. \qquad (18)$$

It turns out that the retrieval by this formula is possible not only for the turbulence with $\gamma = 4$ but also for the turbulence with $\gamma = 11/3$. In this process, the function $f(x)$ should be still defined as $f(x) = q(x)/q_0(x)$, where the functions $q(x)$ and $q_0(x)$ are calculated for a medium with the index $\gamma = 11/3$. The check demonstrated that formula (18) is applicable in the case of receivers whose aperture radii exceed 1 cm. Noticeable distinctions are observed only for aperture radii less than 0.1 cm.

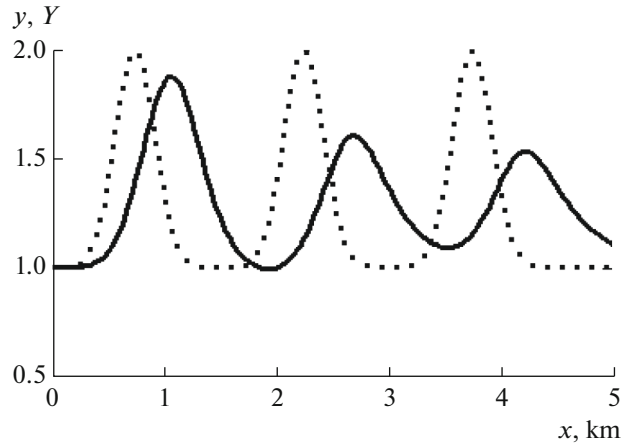

Fig. 7. Distributions: y, specified by formula (16) (dotted curve), and Y, retrieved by formulas (12) and (13) (solid curve). The functions $f(x)$ in these formulas were calculated for $R = 2$ cm.

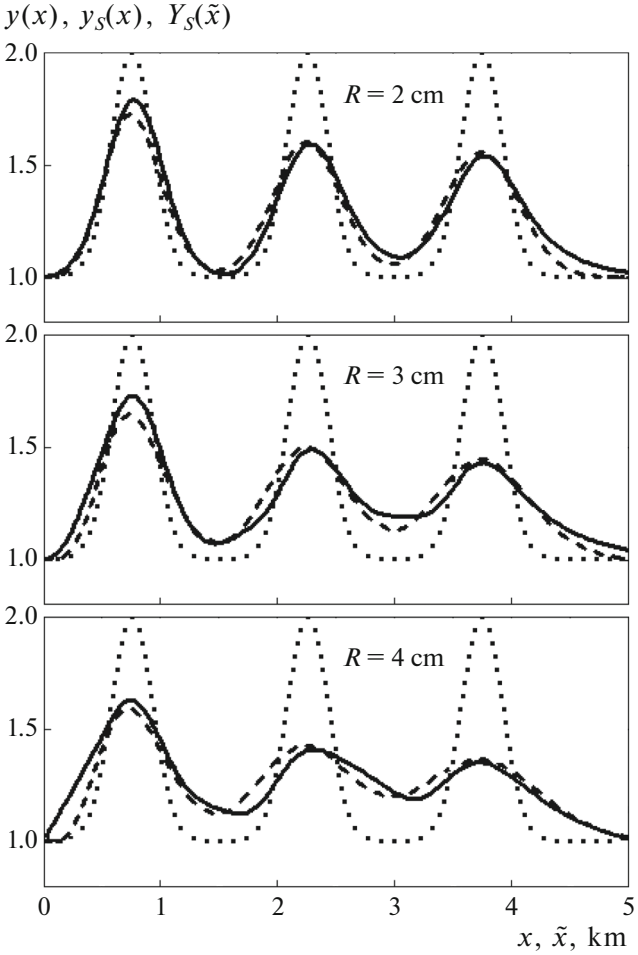

Fig. 8. Given distributions $y(x)$ (dotted curves) and $y_S(x)$, distributions $y(x)$ smoothed by a Gaussian window with a variable width (dashed curves); retrieved distributions $Y_S(\tilde{x})$ smoothed by a window with the constant width $S_Y = 300$ m as functions of the coordinate $\tilde{x}$ defined by formula (17) (solid curves).

CONCLUSIONS

It has been shown that if formulas for retrieving the distribution of the structure parameter $C_n^2(x)$ by data from measurements of the backscattering enhancement factor are based on the geometrical optics asymptotics of the kernel of the integral equation, they are applicable only on short paths with an extension of about 0.5 and 1 km when the radius of the receiving aperture is 10 and 20 cm, respectively. These extensions are less by a factor of hundreds than the corresponding diffraction lengths $L_d = (2\pi/\lambda)R^2$ which are equal to approximately 100 and 400 km at $\lambda = 0.53$ μm. The restrictions are caused by small kernel oscillations which lead to strong oscillations of the third derivative of the measurement data.

Similar formulas based on the asymptotic formula of the kernel for a point receiver are less sensitive to oscillations of the measured data since they include derivatives of order not higher than two. Applying the formulas for a point receiver in the case of receivers with a finite radius leads to smoothing of the retrieved distributions and their shift with respect to the given ones. These factors are regular and easy to take into account when interpreting the results of retrieving the measurement data with receivers whose radius does not exceed 4–5 cm.

Together with smoothing of the retrieved data, applying the point receiver approximation leads to a partial loss of the information about the index of the turbulence spectrum in the retrieved data. This allows one to retrieve the measurement data with the index $\gamma = 11/3$ by the simple formula (18).

ACKNOWLEDGMENTS

I am grateful to V.A. Banakh, M.E. Gorbunov, A.S. Gurvich, and I.G. Yakushkin for the discussions and constructive feedback.

This work was supported by the Russian Foundation for Basic Research (project no. 12-05-00332).

REFERENCES

1. V. V. Vorob'ev, "On the applicability of asymptotic formulas of retrieving "optical" turbulence parameters from pulse lidar sounding data: I–Equations," Atmos. Ocean. Opt. **30** (2), 156–161 (2016).
2. A. S. Gurvich, "Lidar sounding of turbulence based on the backscatter enhancement effect," Izv., Atmos. Ocean. Phys. **48** (6), 585–594 (2012).
3. A. S. Gurvich, "Lidar positioning of higher clear-air turbulence regions," Izv., Atmos. Ocean. Phys. **50** (2), 143–151 (2014).
4. V. A. Banakh and I. A. Razenkov, "Aerosol lidar for study of the backscatter amplification in the atmosphere. Part II. Construction and experiment," Opt. Atmos. Okeana **28** (2), 113–119 (2015).
5. V. A. Banakh and I. A. Razenkov, "Lidar measurements of atmospheric backscattering amplification," Opt. Spectrosc. **120** (2), 326–334 (2016).

Translated by A. Nikol'skii